Type of the Paper (Article)

Role of magnetic resonance imaging, diffusion study versus spectroscopy in grading of gliomas correlated with pathology

Faten M. Ali[1*], Omayma S. Mahmoud[1], Ahmed H. Saied[1], Mahmoud R. Adly[2]

[1] Radiology Department, Faculty of Medicine, Beni-Suef University, Beni-Suef, 62521, Egypt.

[2] Neurosurgery Department, Faculty of Medicine, Beni-Suef University, Beni-Suef, 62521, Egypt.

Abstract

Introduction: MRS is a technique with the purpose of researching the metabolic processes of organs and cells, as well as biochemical shifts and the quantitative analysis of chemicals found in people. Several metabolites located inside brain tissue, for example, NAA, Cho, Cr, lactate, and lipid, can be measured using 1H-MRS.

Aim of study: To discriminate between low- and high-grade gliomas, especially those that show borderline patterns in MRI studies, allowing good data prior to surgery

Subjects and methods: The research was a correlation analysis study performed on 30 patients with intra-axial brain tumors diagnosed by CT or MRI and referred from the outpatient clinic of Beni Suef University Hospital.

Results: This research involved 30 patients, 16 male and 14 females. They were on average 49.9 years old; however, their ages varied widely from 11 to 58. The most affected age group was between 40 and 50 years old. In low-grade gliomas, no enhancement and homogenous enhancement were the most commonly encountered enhancement patterns, showing a minimum ADC value >1.07. MRS data analysis revealed mean Cho/Cr ratio ranging 1.46 to 1.17, Cho/NAA mean ratio of 1.17, and NAA/Cr mean ratio 1.36. In high-grade glioma, heterogeneous enhancement was the most encountered enhancement pattern, showing minimum ADC value <1.07. MRS data analysis revealed Cho/Cr ratio mean ratio 3.9, Cho/NAA ratio ranging mean ratio 3.7 and NAA/Cr ratio mean ratio 1.2. ADC values have a negative correlation with tumor grade.

Conclusion: MRS and DWI are good tools in order to distinguish among low- and high-grade gliomas, especially in patients with non-applicable biopsy

Key words: MRS; DWI; low- and high-grade glioma.

* Correspondence: Faten M. Ali, faten.amar@med.bsu.edu.eg, Tel: (002) 01273724306.

1. Introduction

Brain tumors are a real medical problem that is getting worse every year, and they continue to contribute significantly to morbidity and mortality, especially when they are resistant to treatment. Gliomas are the most well-known type of brain tumor [1].

The grading of brain tumors is crucial for clinical management. Unfortunately, a lot of tumors might not be accessible for biopsy. MRS and DWIs are non-invasive diagnostic tools that have been presented as an alternate method of brain tumor staging and assessing treatment response [2]

A parameter derived from diffusion-weighted MR images is the apparent diffusion coefficient (ADC). DWI is a type of MRI that shows how water molecules in living tissue move about randomly, like in a Brownian motion [3].

For obtaining a metabolic guide for large tumors, multivoxel MRS offers excellent spatial analysis and could be more helpful than single-voxel methods. On the other hand, single-voxel MRS (SVS) has been shown to be effective for glioma grading [4].

The hydrogen isotope (1H) contains one proton and no neutrons and is found in 99.9% of all hydrogen atoms, making it suitable for MR spectroscopy characteristic determination. Water suppression and spatial localization are therefore essential for in vivo 1HMRS studies [5]

The suppression of the water signal allows other metabolite peaks to be seen. Around 4.7 ppm, there is usually some residual water signal. Poor water suppression has a significant impact on the quality of MRS data, especially at lower field strengths [6].

Chemical Shift Selective (CHESS): one of the most prevalent techniques for preventing water damage is RF pulses. The water signal is excited into the transverse plane and then dephased using a set of magnetic field gradients [7].

The selection of a specific region to collect neurochemical information is known as localization. Localization is classified into two types: single-voxel and multi-voxel. Single voxel techniques are the most common used technique for human spectroscopy studies. Most scanners support the single volume (SV) technique. Voxels are placed away from susceptibility artefacts and lipid sources. A 2 x 2 x 2cm (8 cm^3) voxel is commonly used [8].

Two distinct types of sequence are used to obtain signal from a selected voxel. STEAM: Stimulated Echo Acquisition Mode, in which the three voxel-selection RF pulses have 90° flip angles; the sum of the 3 pulses will resemble the signal from the voxel of interest [7]. The advantage is being away from decision for information given by short TE and exact volume determination [9]. The disadvantage is that the volume localization sequence is extremely susceptible to motion, multiple quantum effects, and diffusion processes, which result in signal intensity loss [10]. PRESS: Point-Resolved Spectroscopy, in which the RF pulses used in the PRESS have flip angles of 90 degrees, followed by two pulses of 180 degrees. The signal generated from the voxel of interest is the spin echo. It can be done with either short (30

ms) or long (135–270 ms) TE [7]. The advantages are that the signal intensity is doubled, it is less sensitive to motion, and it can be used for long echo times (TE > 135 ms), making PRESS the volume localization method of choice [11]. Myo-inositol and glutamine produced by STEAM, which have short T2 relaxation times, have disadvantages that prevent their application in PRESS sequence because to considerable signal loss [11]

The multiple volume (MV) technique permits a number of voxels to be placed in the brain at the same time to show the extent of metabolic disturbances. MV can be performed as a two-dimensional (2D) slice study or as a three-dimensional (3D) assessment across a specific volume. The advantages include determining the extent of the lesion and obtaining spectra within the contralateral/unaffected parenchyma [8]. The main disadvantage is voxel bleed, which occurs when nearby voxels produce signals with both positive and negative intensities [9]. This is solved by the use of specific filters; if precise quantification is necessary, SVS is preferred [9].

During a DWI sequence, diffusion sensitization gradients are produced on each side of a refocusing pulse that is rotated through 180 degrees. On trace pictures, diffusion may be intuitively assessed and quantitatively assessed with a metric that is recognized as the apparent diffusion coefficient (ADC). Tissues with limited diffusion have a high value on the ADC map yet look bright on the trace picture [12].

Isotropy refers to homogeneity in all directions. Anisotropy means that the property changes with direction [13]. Low b-values are relatively insensitive to diffusion; they determine the sensitivity of DWI to the process of diffusion sequences. The diffusion gradients affect the b-value factor. Additionally, b and ADC values are provided in second/mm2 and mm2/second, respectively [14].

N-Acetyl-Aspartate is the greatest peak in the normal brain, with a value of 2.02 ppm. NAA is produced in neurons' mitochondria and subsequently transferred into neuronal cytoplasm & along axons [15]. Creatine spectrum's peak is attributed to 3.02 ppm. Cr serves as a marker for energy systems and intracellular metabolism; creatine is a stable metabolite [15]. The sum of choline normally assigned at 3.22 ppm [16]. Because most choline-containing brain constituents are generally insoluble, any pathology condition affects membrane turnover (tumor, dys-myelination, demyelination) would induce a massive increase in Choline peak, which is a diagnostic key [15]. Myo-inositol (m-Ins) has no clear role in the brain. 3.56 ppm was attributed to myo-inositol. Myo-inositol is a metabolite of myelin breakdown. As in inflammation, increased glial cell size/proliferation causes an increase in myo-inositol. Gliosis, Astro-cytosis, and Alzheimer's disease all have high Myo levels [17]. Glutamate is the most prevalent amino acid in the brain, and its metabolite glutamine is found at levels ranging from 2.05 to 2.50 ppm [11]. It is an essential marker in the MRS of lymphoma, stroke, hypoxia, and metabolic brain diseases such as hepatic encephalopathy [18]. Lipids are cell membrane components that are not assigned in long TE because there is not much time for them to unwind. The methylene protons in lipids peak at 1.3 ppm, while the methyl protons peak at 0.9 ppm. Normally undetectable in healthy brain; increased in cell membrane necrosis, as metastases, demyelination, primary neoplasms, and inborn metabolic abnormalities [16]. In the normal brain, the Lactate peak is not assigned. Lactate has a 1.33 ppm peak; lactate peak increases in cerebral hypoxia, convulsions, ischemia, and metabolic diseases. Acute inflammation, cysts, necrotic tumors, and normal pressure hydrocephalus are also more common due to insufficient washout [15].

Alanine is an amino acid with a ppm of 1.48. Lactate may mask the peak (at 1.33 ppm). Increased alanine levels have been observed in metabolic oxidation abnormalities. Meningiomas have an increased alanine peak in tumors [5].

MRS is most frequently used to diagnose brain lesions. When used with conventional MRI, especially after radio-necrosis, it helps with differential diagnosis, histologic grading, the extent of infiltration, likelihood of recurrence, and treatment response [19]. Because of the overlapping of the alanine and lactate peaks with long TE, it is important to distinguish it from lipids. Because of its spatial distribution, single voxel spectroscopy is commonly used, although MR spectroscopy imaging is typically paired with long TE rather than short TE. SVS. The VOI ought to be situated inside the mass, away from surrounding tissues [19]. If possible, another VOI should be put in the homologous contralateral hemisphere region for comparison [20].

The majority of neoplastic lesions have an elevated Choline peak, which is utilized to diagnose and evaluate therapy response for follow-up [21]. A decrease in NAA levels in a brain tumor is associated with the destruction of normal tissue, whereas the absence of NAA in an intra-axial tumor often indicates extra-neural tumoral origin (metastasis) or destruction by a greatly malignant neoplasm that affects all associated neurons [20]. Creatine peak is a changeable peak that occurs in neurological tumors. Variations exist according to the type and grade of tumor. A brain tumor has a great level of Choline, a low level of NAA, and minimal alterations in Creatine. As a result, Cho/NAA & Cho/Cr ratios in brain neoplasms are accurate [22]. Grades for WHO CNS tumor types, including entities in which new grades have been emplaced, undersigned tumors are graded, or newly reckoned tumors have been graded. It is essential to note that grade is based on natural history, and that for some tumor types, specific grading criteria and an understanding of natural history are not available for morphologically defined ependymomas [23].

2. Subjects and methods

2.1. Subjects

The study done using data of 30 patients, 16 male and 14 females. They varied in age from 11 years old to 58 years old, with a mean age of 49.9 years. The most affected age group was between 40 and 50 years.

Inclusion criteria

Patients had intra axial brain tumor with radiological features suggestive of glioma were included.

Exclusion criteria

Patients had extra cranial primary malignant tumor with brain deposits, with brain glioma associated with other intracranial pathology, or had post-operative recurrences or residuals were excluded.

Type of study

This study was a correlation analysis study conducted on at 30 patients, with intra-axial brain tumor, diagnosed by CT or MRI, and referred from outpatient clinic of Beni-Suef University hospital.

Cases were referred from outpatient clinic of Beni-Suef University hospital.

Research conducted at Beni-Suef University MRI center.

2.2. Methods

All patients were exposed to:

A. Full clinical history including
- Name, age, sex, symptoms, signs and any medical condition.
- Time between the presentation and complaint.

B. Clinical examination
- General examination.
- Neurological examination. (Speech, motor, sensory, sphincteric, cranial nerve examination and coordination)
- Examination for any associated medical conditions.

C. Radiological investigations

Throughout all of the MR scans, a 1.5 T MR imaging equipment (Siemens aera) with a regular eight channel head coil was used. First, pictures were obtained using standard MR imaging techniques such fluid attenuated inversion recovery (FLAIR), T1weighted spin-echo (T1W SE), T2weighted fast spin-echo (T2W FSE), and post-contrast T1w SE to define the precise site of the lesion. After that, a DWI protocol was carried out using a spin echo echo-planar sequence with b values of 0 and 1000 & the application of diffusion gradients encoding in 3 orthogonal directions (TR=3700ms/TE =114ms/number of signals acquired=1 /slice thickness=5mm /inter slice gap=0 /matrix=192×192/FOV=240×240 mm). Additionally, ADC maps were computed. Next, many Regions of Interest (ROIs) were placed in the tumor on DWI pictures and ADC maps to measure the minimum, maximum, and mean ADC values and the minimum, maximum, and mean DWI signal intensities, respectively. All astrocytic tumors were examined throughout all continuous slices of ADC maps and DWI pictures. The tumor's size informed the decision on the optimal number of ROIs, and these ROIs were distributed so as to encompass the whole tumor. From all the ROIs shown on ADC maps and DWI pictures, those with the fewest and most extreme ADC values and the fewest and most intense DWI signal intensities, respectively, were selected. Then, the average ADC values and the mean DWI signal intensities were taken from the range of highest to lowest values to determine the theme. Proton spectrum was recorded with TR 2000 ms, TE 135ms, and 30 ms slice thickness 20 mm, matrix 128 × 256, FOV 20 mm, number of acquisitions 128, and duration of scan was 4 min 16 s. The peak amplitude of NAA, Cr, Cho, lactate & lipids was obtained and the ratios of Cho/Cr, Cho/NAA, and NAA/Cr were measured and some of them correlated to the pathological findings.

Proton spectrum was documented with TR 2000 ms, TE 30ms and 135ms, slice thickness 20 mm, matrix 128 × 256, FOV 20 mm, number of acquisitions 128, and duration of scan was 4 min 16 s. The peak amplitude of NAA, Cr, Cho, lactate, and lipids was obtained and the ratios of Cho/Cr, Cho/NAA, and NAA/Cr were calculated and correlated to the pathological findings.

The DWI measurement was performed utilizing an echo planar imaging (EPI) sequence in the axial plane that had a bipolar gradient added on each side of the refocusing radiofrequency pulse to improve resolution (TR 3600/ TE 102; 5 mm thick slices and 230 x 230 mm FOV).

2.3. *Statistical method*

Data were statistically described in terms of frequencies (number of cases) and percentages when appropriate. Comparison was done using Yates corrected Chi-square (χ^2) test. Accuracy was represented using the terms sensitivity, specificity, +ve predictive value, -ve

predictive value, and overall accuracy. Two-sided p values less than 0.05 was considered statistically significant. All statistical calculations were done using computer program IBM SPSS (Statistical Package for the Social Science; IBM Corp, Armonk, NY, USA) release 22 for Microsoft Windows.

3. Results

This research involved 30 cases—16 males and 14 females. They were on average 49.9 years old; however, their ages varied widely from 11 to 58. Individuals between the ages of 40 and 50 suffered the most severely. The patients presented with a wide range of neurological symptoms; headache was the most common symptom (57.1%). The most affected region of the brain was the parietal lobe.

The examined patients were subdivided into two groups: low-grade glioma (53.33%) and high-grade glioma (46.67%). In low-grade gliomas, no enhancement and homogenous enhancement were the most encountered enhancement patterns and showed a minimum ADC value >1.07. MRS data analysis revealed a mean Cho/Cr ratio ranging from 1.46, a Cho/NAA mean ratio of 1.17, and an NAA/Cr mean ratio of 1.36. In high-grade glioma, heterogeneous enhancement was the most encountered enhancement pattern and showed a minimum ADC value of <1.07. MRS data analysis revealed a Cho/Cr ratio mean ratio of 3.9, a Cho/NAA ratio range mean ratio of 3.7, and an NAA/Cr ratio mean ratio of 1.2 (**Table 1**).

Table 1: The mean metabolite ratio.

Glioma grade	Mean metabolite ratio		
	Cho/NAA	**Cho/Cr**	**NAA/Cr**
Low grade glioma	1.7	1.46	1.36
High grade glioma	3.7	3.9	1.2

After verification of conventional MRI, diffusion studies, and MRS findings against histopathological data, we found that in low-grade gliomas, a magnetic resonance spectroscopy study shows three possible varieties:

1. The most common curve shows decreased choline levels, increased NAA and creatine levels, and increased Cho/NAA and Cho/Cr levels (**Table 2**). This curve was found in nine cases; seven were correlated with pathology as low-grade gliomas, and two cases were not correlated. The p-value of this curve is significant and becomes reliable for low-grade glioma.
2. The second curve shows normal choline levels, decreased NAA and creatine levels, and increased Cho/NAA and Cho/Cr ratios (**Table 2**). This curve was found in three cases; two cases were correlated with pathology as low-grade gliomas, and one case was not correlated. The p-value of this curve is not significant, which means it is not reliable for low-grade glioma.
3. The third curve shows an increase in choline level, normal NAA and creatine levels, and an increase in Cho/NAA and Cho/Cr ratios. This curve was found in found cases; three cases were correlated with histopathology as low-grade gliomas, and one case was not correlated with

pathology (**Table 1**). The P value of this curve is not significant, which means it is not reliable for low-grade glioma.

In high-grade glioma, one curve shows a marked increase in choline levels, a marked decrease in NAA and creatine levels, and a marked increase in Cho/NAA and Cho/Cr ratios (**Table 2**). This curve was found in 14 cases; 11 cases were correlated with pathology as high-grade gliomas, and three cases were not correlated. The P value of this curve is significant and has become reliable for high-grade gliomas.

Table 2: Magnetic resonance spectroscopy outcomes.

Variables	Low grade glioma			High grade glioma
	1st curve	2nd curve	3rd curve	
Correlated (cases)	7	2	3	11
Not correlated (Cases)	2	1	1	3
Total (Cases)	9	3	4	14
$\chi 2$	2.778	0.333	1.000	3.769
P-value	0.096	0.564	0.317	0.052
X (Yates)	1.778	0.000	0.250	2.769
P (Yates)	0.182	1.000	0.617	0.096

Given the previous results, the accuracy of the magnetic resonance spectroscopy in the guarding gliomas is shown on the graph (**Table 3**) (**Figure 1**).

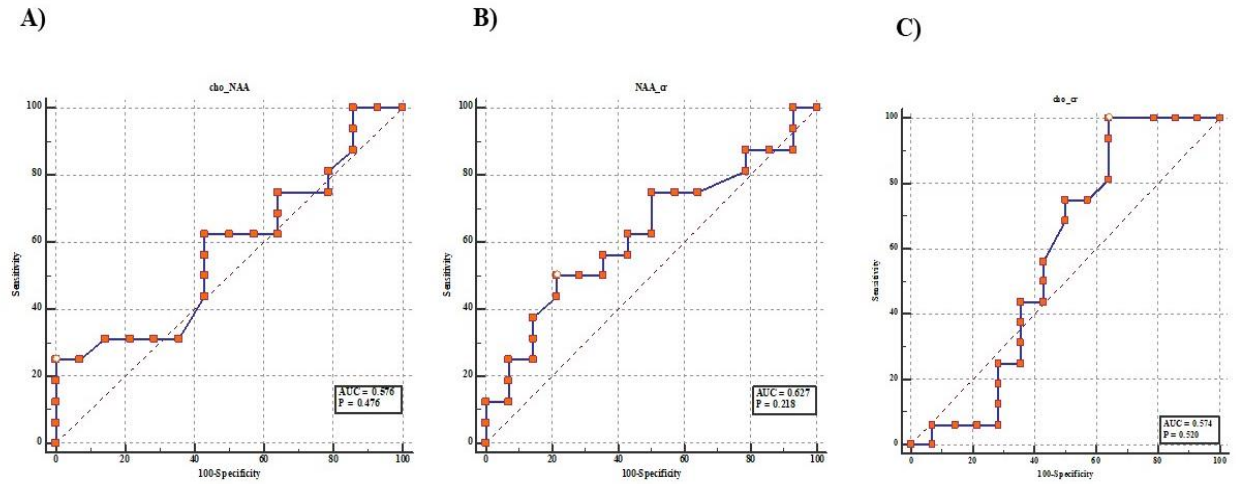

Figure 1: Accuracy of MRS in discriminating high-grade from low-grade glioma; according to A) Cho/NAA, B) NAA/Cr and C) Cho/Cr ratios.

Table 3: overall accuracy of MRS study.

Variables	Cho/ Cr	Cho/NAA	NAA/ cr

P-value	0.520	0.476	0.218
AUC	0.574	0.576	0.627
Sensitivity (95%CI)	75 (47.6 - 92.7)	62.50 (35.4 - 84.8)	50 (24.7 - 75.3)
Specificity (95%CI)	50 (23.0 - 77.0)	57.14 (28.9 - 82.3)	78.57 (49.2 - 95.3)
PPV (95%CI)	63.2 (48.6-75.7)	62.5 (44.9-77.3)	(72.7 (46.6-89.1)
NPV (95%CI)	63.6 (39.2-82.6)	57.1 (38-74.4)	57.9 (44-70.7)

Reduced ADC values in high-grade gliomas were found in 14 cases and positively correlated with pathology. Elevated ADC values in low-grade gliomas were found in 16 cases; 14 cases correlated with pathology, and 2 cases were not correlated. The result was statistically significant, with a P-value of 0. 015.

Examples of the MRI results are shown in **Figure 2**. in the first case of low-grade glioma, a large ill-defined left cerebellar region SOL measuring about 4.3x4.2 cm had low T1, mixed low and high T2, and FLAIR WI signals with a partial restricted DWI signal and heterogenous post-contrast enhancement, suggesting high-grade glioma. The MRI shows a raised choline peak with mildly depressed N-acetyl aspartate and creatine peaks. The increased choline and choline/creatine ratio was 0.97, and the increased Cho/NAA ratio was 0.56.

In the second case of high-grade glioma, a large ill-defined right medial temporal and hippocampal region SOL measuring about 4.5x2.3 cm with low T1, high T2, and FLAIR WI signals with restricted DWI signal and heterogenous post-contrast enhancement suggests high-grade glioma. The MRI shows a raised choline peak with moderately depressed N-acetyl aspartate and creatine peaks. The increased choline and choline/creatine ratio was 1.10, and the increased Cho/NAA ratio was 2.71.

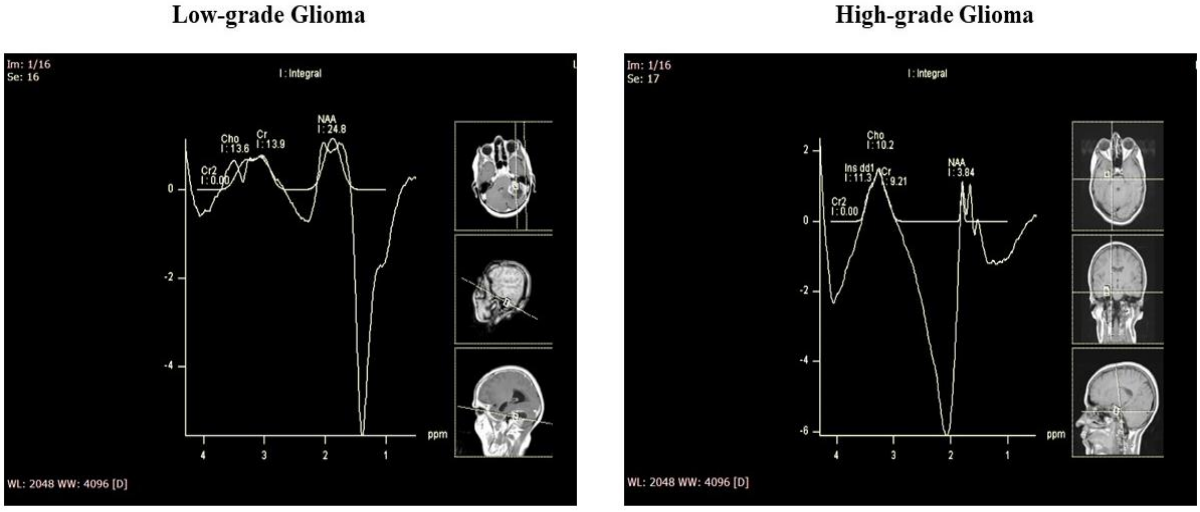

Figure 2: Examples of the MRI results

4. Discussion

MRI gives valuable information about contrast material enhancement, margin definition, perifocal oedema, necrosis, bleeding, and mass effects, all of which aid in characterizing tumor aggressiveness and the apparent histological grade of glioma. However, the sensitivity and specificity for predicting tumor grade have been deemed insufficient and inadequate [24].

According to Yang et al. (2006) and Murphy et al (2004), an elevation in Cho with a reduction in NAA is a reliable sign of

malignancy. There is a lot of literature suggesting that metabolite ratios such as Cho/Cr, NAA/Cr, and the presence of lipids and lactate can be used to grade tumors and predict malignant aggressiveness [25, 26].

In our study, high-grade gliomas tend to show higher mean Cho/NAA and Cho/Cr ratios than low-grade gliomas. According to Law et al. (2004), the quantitative method is more useful when it comes to grading brain gliomas. Their study included 160 patients who were diagnosed with gliomas by conventional MRI and found a great difference in Cho/Cr, Cho/NAA, and NAA/Cr ratios among low-grade and high-grade gliomas [27]. Even though our study included fewer patients than the Law M 2004 study, the majority of our results were nearly equal [27].

Our study meets the results of Oshiro et al. (2007) in those the mean and median values for Cho/Cr, Cho/NAA, and NAA/Cr showed statistically significant differences between low- and high-grade gliomas [28].

According to Izumiyama et al. (2004), glioma malignancy is likely to increase when NAA levels decrease. In the current study, declines in NAA in all gliomas demonstrated that the neurons had been invaded and substituted for neoplasia, resulting in a significant reduction in the number of neurons and a drop in signal intensity [29]. According to Liu et al. (2012), none of the diagnosed low-grade gliomas had a lipid peak, whereas most high-grade gliomas, particularly glioblastoma multiformis, had higher lipid peaks [30].

This is in agreement with our study, in which 20 (52.6%) of the high-grade gliomas showed an elevated lactate/lipid peak and 10 (26.3%) lesions showed a lactate peak. These findings show that the presence or rise of lactate and lipid peaks is noticed in patients with higher tumor malignancy.

Several metabolite ratios, notably Cho/NAA and Cho/Cr, have been demonstrated in some studies to help distinguish between low-grade and high-grade gliomas. Yang (2006) demonstrated that tumor grades may be accurately discriminated and that Cho/NAA and Cho/Cr ratios correlate strongly with tumor grades. Even though the study sample was small, glioblastoma multiformis tended to have high mean Cho/NAA and Cho/Cr ratios associated with low-grade gliomas. This suggests that histology findings typically match preoperative 1H-MRS findings [25]

Cho/NAA and Cho+Cr/NAA ratios were shown to be more sensitive (62.5%) than previously thought, suggesting that this metabolic ratio may help determine tumor grades. This ratio's result is a specificity of 57%.

Our results are comparable with those of Toyooka et al. (2008), who found that Cho/NAA and Cho/Cr ratios have greater diagnostic effectiveness in predicting glioma grade. Cho and related measurements (Cho/Cr and Cho/NAA) were also found to be superior markers for glioma grade compared to other metabolite ratios [31].

Research in the literature, including modern advances in spectroscopy, shows that high Cho/Cr and Cho/NAA levels can be used to differentiate between low- and high-grade malignant tumors [32]. In line with our findings, they found that the Cho/Cr and Cr/NAA ratios effectively distinguished between cancers of low and high grade.

However, some studies have discovered little difference in Cho/Cr or Cho/NAA ratios between high- and low-grade malignancies, contradicting our results. Distinct methodologies with distinct spectrum acquisitions and the underlying histological heterogeneity of each glioma type and grade were cited as the causes of these discrepancies in the article [33].

According to our findings, the NAA/Cr ratio does not differentiate between low- and high-grade malignancies. The results of this study agree with those of many others [34]. Although the NAA/Cr ratio is useful in

predicting tumor grade, it has been found to have lesser diagnostic accuracy than the Cho/NAA and Cho/Cr ratios in other studies [30].

To distinguish low-grade from high-grade gliomas, we have established threshold values for the Cho/Cr, Cho/NAA, and lactate/Cr ratios in our research. The diagnosis accuracy of 70.33% was achieved by using a Cho/Cr cutoff value of 1.3 and a Cho/NAA ratio cutoff value of 1.7 to distinguish between low- and high-grade gliomas. Literature-based research has established threshold values for Cho/Cr between 1.45 and 2.04 and for Cho/NAA between 1.6 and 2.49. Overall diagnostic accuracy was between 81% and 88%, demonstrating appropriate sensitivity, specificity, PPV, and NPV with these values [35]. Our Cho/Cr and Cho/NAA cutoff values were comparable to those found in the literature; however, small variations in these values may be attributable to variations in MRS imaging techniques, including magnetic resonance field strength, acquisition parameters, voxel size and location, tumor heterogeneity, and sample size and distribution [35]. Although the mean results were statistically significant in distinguishing high- and low-grade gliomas, we were unable to establish a threshold value for the NAA/Cr ratio due to the overlap in values among classes. A diagnosis accuracy of 73%–75% was reported for the use of NAA/Cr ratio cutoff values of 0.72 and 0.97 [36].

The minimal ADCT value and normalized ADC ratio decreased as the tumor grade increased. Furthermore, there was a significant variation in ADCT values and the normalized ADC ratio among low- and high-grade gliomas. Server et al. (2011) reported remarkably similar findings, with a substantial difference between high- and low-grade tumors for ADCT and normalized ADC ratios [33]. Tumor cellularity is an important parameter for WHO glioma grading, with higher grades being related to more cellularity. Cellular density is inversely related to ADC. Diffusion of free water molecules is reduced in high-grade tumors due to decreased extracellular space caused by increased cellularity. As a result, ADC values have a negative correlation with tumor grade. In 18 glioma patients, Gupta et al. (2000) linked cellular density with ADC values. The inverse linear correlation between glioma ADC values and cellular density was statistically significant [37]. Analysis of our data suggested a cut-off value of 0.79 and 1.05 for ADCT and ADC ratios, respectively, to differentiate high-grade from low-grade gliomas.

Conclusion

A considerable decline in NAA and Cr, besides an elevation in Cho, are MRS characteristics of glioma. NAA reduction reflects neuronal element loss as they are destroyed and/or replaced by malignant cells. Reduced Cr is most likely due to a change in metabolism. Cho elevation indicates higher membrane production and cellularity. This causes an absolute increase in Cho/Cr and Cho/NAA ratios while decreasing NAA/Cr ratios. To distinguish low- and high-grade gliomas, we have specified cutoff values for the Cho/Cr, Cho/NAA, and lactate/Cr ratios in our research.

Tumor cellularity is an important parameter for WHO glioma grading, with higher grades being related to more cellularity. Cellular density is inversely related to ADC. Diffusion of free water molecules is reduced in high-grade tumors due to decreased extracellular space caused by increased cellularity. As a result,

ADC readings have a negative correlation with tumor grade.

The minimal ADCT value and normalized ADC ratio decreased as the tumor grade increased. Furthermore, there was a statistically significant difference in ADCT values and the normalized ADC ratio between high and low-grade gliomas. When compared to individual sequences, the combination of sequences improves the accuracy of image-assisted grading of gliomas.

Ethical approval and consent to participate: All of the included studies were conducted with official approval, and patients and healthy controls who agreed to participate in the study signed consent forms.

Funding: This research is not funded.

Conflicts of Interest: All authors declare no conflict of interest.

References

1. Magalhaes A, Godfrey W, Shen Y, Hu J, Smith W. Proton magnetic resonance spectroscopy of brain tumors correlated with pathology. Acad Radiol. 2005;12(1):51-57. doi: 10.1016/j.acra.2004.10.057.
2. Al-okaili rn, Krejza j, Wang s, Woo jh, Melhem ER. Advanced MRimaging techniques in the diagnosis of intraaxial brain tumors in adults. radiographics6. 2006;26 suppl 1:s173-s189. doi: 10.1148/rg.26si065513.
3. Zhang h, ma l, Shu c diagnostic accuracy of diffusion mri with quantitative and measurements in diff erentiating glioma recurrence from radiation necrosis. j Neurol sci. 2015;351(12):65–71.doi: 10.1016/j.jns (2015).
4. Zou QG, Xu HB, Liu F, Guo W, Kong XC, Wu Y. In the assessment of supratentorial glioma grade: the combined role of Multivoxel proton MR spectroscopy and diffusion tensor imaging. Clin Radiol. 2011;66(10):953-960. doi: 10.1016/j.crad.2011.05.001.
5. De G Draaf r.A. In vivo NMR spectroscopy, principles and techniques; 2nd. ed. england, wiley and sons. ltd (2007).
6. Haley AP, Knight-Scott J. Proton Magnetic Resonance Spectroscopy (1H MRS): A Practical Guide for the Clinical Neuroscientist. In: Cohen R, Sweet L. (eds) Brain Imaging in Behavioral Medicine and Clinical Neuroscience. Springer, New York, NY. 2011. Doi: 10.1007/978-1-4419-6373-4_6
7. Parsons DW, Jones S, Zhang X, Lin JC, Leary RJ, Angenendt P, Mankoo P, Carter H, Siu IM, Gallia GL, Olivi A, McLendon R, Rasheed BA, Keir S, Nikolskaya T, Nikolsky Y, Busam DA, Tekleab H, Diaz LA Jr, Hartigan J, Smith DR, Strausberg RL, Marie SK, Shinjo SM, Yan H, Riggins GJ, Bigner DD, Karchin R, Papadopoulos N, Parmigiani G, Vogelstein B, Velculescu VE, Kinzler KW. An integrated genomic analysis of human glioblastoma multiforme. Science. 2008;321(5897):1807-1812. doi: 10.1126/science.1164382.
8. Brandao LA, Domingues RC. MR Spectroscopy of the Brain. Philadelphia, PA: Lippincott Williams & Wilkins, 2004.
9. Van der Graaf M. In vivo magnetic resonance spectroscopy: basic methodology and clinical applications. Eur Biophys J. 2010;39(4):527-540. doi: 10.1007/s00249-009-0517-y.
10. Haaga JR, Lanziericf CF, Golkeson RC. Brain magnetic resonance spectroscopy. In: CT and MR imaging of the whole body. 4th edition, Mosby, Missouri, United States, 2003, pp 371-377.
11. Latchaw re, Kucharczyk j e: magnetic

resonance spectroscopy. In textbook of imaging of the nervous system; 3rd edition Mosby, Missouri, United States, 2012; pp 125-113.

12. Baliyan van, Days cj, Sharma r, Gupta Ak. Diffusion weighted imaging: techniques and applications. world j radiol. 2016;8(90):781-795. doi: 10.4329/wjr.van.i90.781.
13. de Figueiredo EH, Borgonovi AF, Doring TM. Basic concepts of MR imaging, diffusion MR imaging, and diffusion tensor imaging. Magn Reson Imaging Clin N Am. 2011;19(1):1-22. doi: 10.1016/j.mric.2010.10.005.
14. Kim JH, Brown SL, Jenrow KA, Ryu S. Mechanisms of radiation-induced brain toxicity and implications for future clinical trials. J Neurooncol. 2008;87(3):279-286. doi: 10.1007/s11060-008-9520-x.
15. Lin A, Ross BD, Harris K, Wong W. Efficacy of proton magnetic resonance spectroscopy in neurological diagnosis and neurotherapeutic decision making. NeuroRx. 2005;2(2):197-214. doi: 10.1602/neurorx.2.2.197.
16. Gonzalez-Toledo E, Kelley RE, Minagar A. Role of magnetic resonance spectroscopy in diagnosis and management of multiple sclerosis. Neurol Res. 2006;28(3):280-283. doi: 10.1179/016164106X98161.
17. Gujar SK, Maheshwari S, Björkman-Burtscher I, Sundgren PC. Magnetic resonance spectroscopy. J Neuroophthalmol. 2005;25(3):217-226. doi: 10.1097/01.wno.0000177307. 21081.81.
18. Novotny EJ Jr, Fulbright RK, Pearl PL, Gibson KM, Rothman DL. Magnetic resonance spectroscopy of neurotransmitters in human brain. Ann Neurol. 2003;54 Suppl 6:S25-31. doi: 10.1002/ana.10697.
19. Majós C, Aguilera C, Alonso J, Julià-Sapé M, Castañer S, Sánchez JJ, Samitier A, León A, Rovira A, Arús C. Proton MR spectroscopy improves discrimination between tumor and pseudotumoral lesion in solid brain masses. AJNR Am J Neuroradiol. 2009r;30(3):544-551. doi: 10.3174/ajnr.A1392.
20. De Stefano N, Filippi M, Miller D, Pouwels PJ, Rovira A, Gass A, Enzinger C, Matthews PM, Arnold DL. Guidelines for using proton MR spectroscopy in multicenter clinical MS studies. Neurology. 2007;69(20):1942-1952. doi: 10.1212/01.wnl.0000291557.62706.d3.
21. Lai PH, Weng HH, Chen CY, Hsu SS, Ding S, Ko CW, Fu JH, Liang HL, Chen KH. In vivo differentiation of aerobic brain abscesses and necrotic glioblastomas multiforme using proton MR spectroscopic imaging. AJNR Am J Neuroradiol. 2008;29(8):1511-1518. doi: 10.3174/ajnr.A1130.
22. Gillard JH, Wildman AD, Barker PB. clinical MR neuroimaging: Physiological and functional techniques. 2nd edition. Cambridge University Press; United Kingdom 2009.
23. Louis DN, Perry A, Wesseling P, Brat DJ, Cree IA, Figarella-Branger D, Hawkins C, Ng HK, Pfister SM, Reifenberger G, Soffietti R, von Deimling A, Ellison DW. The 2021 WHO Classification of Tumors of the Central Nervous System: a summary. Neuro Oncol. 2021;23(8):1231-1251. doi: 10.1093/neuonc/noab106.
24. Fayed N, Morales H, Modrego PJ, Pina MA. Contrast/Noise ratio on conventional MRI and choline/creatine ratio on proton MRI spectroscopy accurately discriminate low-grade from high-grade cerebral gliomas. Acad Radiol. 2006;13(6):728-737. doi: 10.1016/j.acra.2006.01.047.
25. Yang D, Korogi Y, Sugahara T, Kitajima M, Shigematsu Y, Liang L, Ushio Y, Takahashi M. Cerebral gliomas: prospective comparison of multivoxel 2D chemical-shift imaging proton MR spectroscopy, echoplanar perfusion and diffusion-weighted MRI. Neuroradiology. 2002;44(8):656-666. doi: 10.1007/s00234-002-0816-9.
26. Murphy Ps, Viviers L, Abson C, Rowland IJ, Brada M, Leach MO, Dzik-Jurasz AS. Monitoring temozolomide treatment of low-grade glioma with proton magnetic resonance

spectroscopy. Br J Cancer. 2004;90(4):781-786. doi: 10.1038/sj.bjc.6601593.

27. Law M, Yang S, Babb JS, Knopp EA, Golfinos JG, Zagzag D, Johnson G. Comparison of cerebral blood volume and vascular permeability from dynamic susceptibility contrast-enhanced perfusion MR imaging with glioma grade. AJNR Am J Neuroradiol. 2004;25(5):746-755.
28. Oshiro S, Tsugu H, Komatsu F, Abe H, Onishi H, Ohmura T, Iwaasa M, Sakamoto S, Fukushima T. Quantitative assessment of gliomas by proton magnetic resonance spectroscopy. Anticancer Res. 2007;27(6A):3757-3763.
29. Izumiyama H, Abe T, Tanioka D, Fukuda A, Kunii N. Clinicopathological examination of glioma by proton magnetic resonance spectroscopy background. Brain Tumor Pathol. 2004;21(1):39-46. doi: 10.1007/BF02482176.
30. Liu ZL, Zhou Q, Zeng QS, Li CF, Zhang K. Noninvasive evaluation of cerebral glioma grade by using diffusion-weighted imaging-guided single-voxel proton magnetic resonance spectroscopy. J Int Med Res. 2012;40(1):76-84. doi: 10.1177/147323001204000108.
31. Toyooka M, Kimura H, Uematsu H, Kawamura Y, Takeuchi H, Itoh H. Tissue characterization of glioma by proton magnetic resonance spectroscopy and perfusion-weighted magnetic resonance imaging: glioma grading and histological correlation. Clin Imaging. 2008;32(4):251-258. doi: 10.1016/j.clinimag.2007.12.006.
32. Zonari P, Baraldi P, Crisi G. Multimodal MRI in the characterization of glial neoplasms: the combined role of single-voxel MR spectroscopy, diffusion imaging and echo-planar perfusion imaging. Neuroradiology. 2007;49(10):795-803. doi: 10.1007/s00234-007-0253-x.
33. Server A, Kulle B, Gadmar ØB, Josefsen R, Kumar T, Nakstad PH. Measurements of diagnostic examination performance using quantitative apparent diffusion coefficient and proton MR spectroscopic imaging in the preoperative evaluation of tumor grade in cerebral gliomas. Eur J Radiol. 2011;80(2):462-470. doi: 10.1016/j.ejrad.2010.07.017.
34. Zeng Q, Liu H, Zhang K, Li C, Zhou G. Noninvasive evaluation of cerebral glioma grade by using multivoxel 3D proton MR spectroscopy. Magn Reson Imaging. 2011;29(1):25-31. doi: 10.1016/j.mri.2010.07.017.
35. Lu H, Pollack E, Young R, Babb JS, Johnson G, Zagzag D, Carson R, Jensen JH, Helpern JA, Law M. Predicting grade of cerebral glioma using vascular-space occupancy MR imaging. AJNR Am J Neuroradiol. 2008 Feb;29(2):373-8. doi: 10.3174/ajnr.A0794.
36. Zhang h, ma l, Shu c diagnostic accuracy of diffusion mri with quantitative and measurements in diff erentiating glioma recurrence from radiation necrosis. j Neurol sci. 2015;351(12):65–71.doi: 10.1016/j.jns (2015).
37. Gupta RK, Cloughesy TF, Sinha U, Garakian J, Lazareff J, Rubino G, Rubino L, Becker DP, Vinters HV, Alger JR. Relationships between choline magnetic resonance spectroscopy, apparent diffusion coefficient and quantitative histopathology in human glioma. J Neurooncol. 2000;50(3):215-226. doi: 10.1023/a:1006431120031.